Supramolecular Chemistry
Publication details, including instructions for authors and subscription information:
http://www.informaworld.com/smpp/title~content=t713649759

Study of the interaction between ruthenium(II) complexes and CT-DNA: synthesis, characterisation, photocleavage and antimicrobial activity studies

K. Ashwini Kumar[a]; Kotha Laxma Reddy[a]; S. Satyanarayana[a]
[a] Department of Chemistry, Osmania University, Hyderabad, Andhra Pradesh, India

Online publication date: 09 October 2010

To cite this Article Ashwini Kumar, K. , Laxma Reddy, Kotha and Satyanarayana, S.(2010) 'Study of the interaction between ruthenium(II) complexes and CT-DNA: synthesis, characterisation, photocleavage and antimicrobial activity studies', Supramolecular Chemistry, 22: 10, 629 — 643
To link to this Article: DOI: 10.1080/10610278.2010.510194
URL: http://dx.doi.org/10.1080/10610278.2010.510194

Supramolecular Chemistry
Vol. 22, No. 10, October 2010, 629–643

Taylor & Francis
Taylor & Francis Group

Study of the interaction between ruthenium(II) complexes and CT-DNA: synthesis, characterisation, photocleavage and antimicrobial activity studies

K. Ashwini Kumar, Kotha Laxma Reddy and S. Satyanarayana*

Department of Chemistry, Osmania University, Hyderabad, Andhra Pradesh 500007, India

(*Received 9 March 2010; final version received 15 July 2010*)

Two polypyridyl ligands 6-fluro-3-(1H-imidazo [4,5-f] [1,10]-phenanthroline-2-yl)-4H-chromen-4-one (FIPC), 6-chloro-3-(1H-imidazo [4,5-f] [1,10]-phenanthroline-2-yl)-4H-chromen-4-one (ClIPC) polypyridyl ligands and their Ru(II) complexes $[Ru(bipy)_2FIPC]^{2+}$(1), $[Ru(dmb)_2FIPC]^{2+}$(2), $[Ru(phen)_2FIPC]^{2+}$(3), $[Ru(bipy)_2ClIPC]^{2+}$(4), $[Ru(dmb)_2ClIPC]^{2+}$(5) and $[Ru(phen)_2ClIPC]^{2+}$(6) ((bipy = 2,2′-bipyridine, dmb = 4,4′-dimethyl-2,2′-bipyridine and phen = 1,10-phenanthroline) have been synthesised and characterised by elemental analysis, Mass spectra, IR, ^1H and ^{13}C-NMR. The DNA-binding of the six complexes to calf-thymus DNA (CT-DNA) has been investigated by different spectrophotometric, fluorescence and viscosity measurements. The results suggest that 1–6 complexes bind to CT-DNA through intercalation. The variation in binding affinities of these complexes is rationalised by a consideration of electrostatic, steric factors and nature of ancillary ligands. Under irradiation at 365 nm, the three complexes have also been found to promote the photocleavage of plasmid pBR 322 DNA. Inhibitor studies suggest that singlet oxygen ($^1O_2$) plays a significant role in the cleavage mechanism of Ru(II) complexes. Thereby, under comparable experimental conditions $[Ru(phen)_2FIPC]^{2+}$(3), $[Ru(phen)_2ClIPC]^{2+}$(6) cleaves DNA more effectively than 1, 2, 4 and 5 complexes do. The Ru(II) polypyridyl complexes (1–6) have been screened for antimicrobial activities.

Keywords: polypyridyl ligand; Ru(II) complexes; DNA-binding; photocleavage; antimicrobial activity

Introduction

The interactions of DNA with transition metal complexes, which contain planar polycyclic hetero aromatic ligands, have been extensively studied (*1*). A number of metal chelates is of current interest for important applications in nucleic acid chemistry as probes of DNA structure in solution, reagents for mediation of strand scission of duplex DNA under physiological conditions and chemotherapeutic agents and in genomic research (*2–5*). The interaction of transition metal polypyridyl and mixed ligand complexes with DNA has been extensively studied during the past several years (*6–11*). The binding of $[Ru(phen)_3]^{2+}$ remains an issue of rigorous debate (*12*, *13*) with factors such as size, shape and planarity of the intercalative ligand, and changing substituent group or substituent position on the intercalative ligand influencing the DNA-binding mechanism (*14–17*). Since octahedral polypyridine Ru(II) complexes bind to DNA in three dimensions, the ancillary ligands also play an important role in the DNA-binding mechanism and behaviours (*18–22*). Recently, our group has reported (*23–27*) binding and photocleavage studies of several mixed ligand complexes of ruthenium(II) and cobalt(III). We chose to concentrate our work on ruthenium(II) complexes of polypyridyls, which have interesting DNA-binding properties. Herein, we report the synthesis and characterisation of 6-fluro-3-(1H-imidazo [4,5-f] [1,10]-phenanthroline-2-yl)-4H-chromen-4-one (FIPC), 6-chloro-3-(1H-imidazo [4,5-f] [1,10]-phenanthroline-2-yl)-4H-chromen-4-one (ClIPC) polypyridyl ligands and their Ru(II) complexes $[Ru(bipy)_2FIPC]^{2+}$(1), $[Ru(dmb)_2FIPC]^{2+}$(2), $[Ru(phen)_2FIPC]^{2+}$(3), $[Ru(bipy)_2ClIPC]^{2+}$(4), $[Ru(dmb)_2ClIPC]^{2+}$(5) and $[Ru(phen)_2ClIPC]^{2+}$(6) ((bipy = 2,2′-bipyridine, dmb = 4,4′-dimethyl-2,2′-bipyridine and phen = 1,10-phenanthroline). In the present study, the DNA-binding behaviour of complexes 1–6 is explored by absorption, emission spectroscopy and viscosity measurements and their abilities to induce cleavage of pBR-322 DNA. Furthermore, all the six Ru(II) complexes synthesised were screened *in vitro* for their antimicrobial activity.

Experimental

Materials

$RuCl_3$, 1,10-phenanthroline monohydrate and 2,2′-bipyridine were purchased from Merck (Mumbai, India). Calf-thymus DNA (CT-DNA), tetrabutylammoniumchloride (TBACl), 6-fluoro-4-oxo-4H-chromene-3-carbaldehyde,

*Corresponding author. Email: ssnsirasani@gmail.com

ISSN 1061-0278 print/ISSN 1029-0478 online

DOI: 10.1080/10610278.2010.510194
http://www.informaworld.com

6-chloro-4-oxo-4H-chromene-3-carbaldehyde, tetrabutylammoniumhexafluorophosphate ($TBAPF_6$) and 4,4′-dimethyl-2,2′-bipyridine were obtained from Sigma (St Louis, MO, USA). The super coiled (CsCl purified) pBR-322 DNA (Bangalore Genie, Bangalore, India) was used as received. All other common chemicals and solvents were procured locally from available sources. All the solvents were purified before use as per standard procedures (*28*). Deionised, double distilled water was used for preparing various buffers. Solutions of DNA in Tris–HCl buffer (pH = 7.2), 50 mM NaCl gave a ratio of UV absorbance at 260 and 280 nm of 1.8–1.9 indicating that the DNA was sufficiently free of protein (*29*). The concentration of CT-DNA (NP) was determined spectrophotometrically using molar absorption 6600 $M^{-1}\,cm^{-1}$ (260 nm) (*30*).

Synthesis and characterisation

The compounds 1,10-phenanthroline-5,6-dione (*31*), $[Ru(bipy)_2Cl_2]$, $[Ru(dmb)_2Cl_2]$ and $[Ru(phen)_2Cl_2]$ were prepared according to the literature procedures (*32*). Synthetic routines of ligands and their Ru(II) complexes are shown in Scheme 1.

Synthesis of ligands

6-Fluro-3-(1H-imidazo [4,5-f] [1,10]-phenanthroline-2-yl)-4H-chromen-4-one. The ligand FIPC was prepared by condensation reaction of 1,10-phenanthroline-5,6-dione (0.260 g, 1.2 mmol), with 6-fluoro-4-oxo-4H-chromene-3-carbaldehyde (0.345 g, 1.8 mmol) in the presence of ammonium acetate (1.9 g, 25 mmol) and 10 ml glacial acetic acid by refluxing for 2 h. The deep red solution obtained was cooled, diluted with water (25 cm^3) and neutralised with ammonia. Then, the mixture was filtered and the precipitate was washed with H_2O and Me_2CO, and then dried (yield: 85%).

6-Chloro-3-(1H-imidazo [4,5-f] [1,10]-phenanthroline-2-yl)-4H-chromen-4-one. The ligand ClIPC was prepared by condensation reaction of 1,10-phenanthroline-5,6-dione

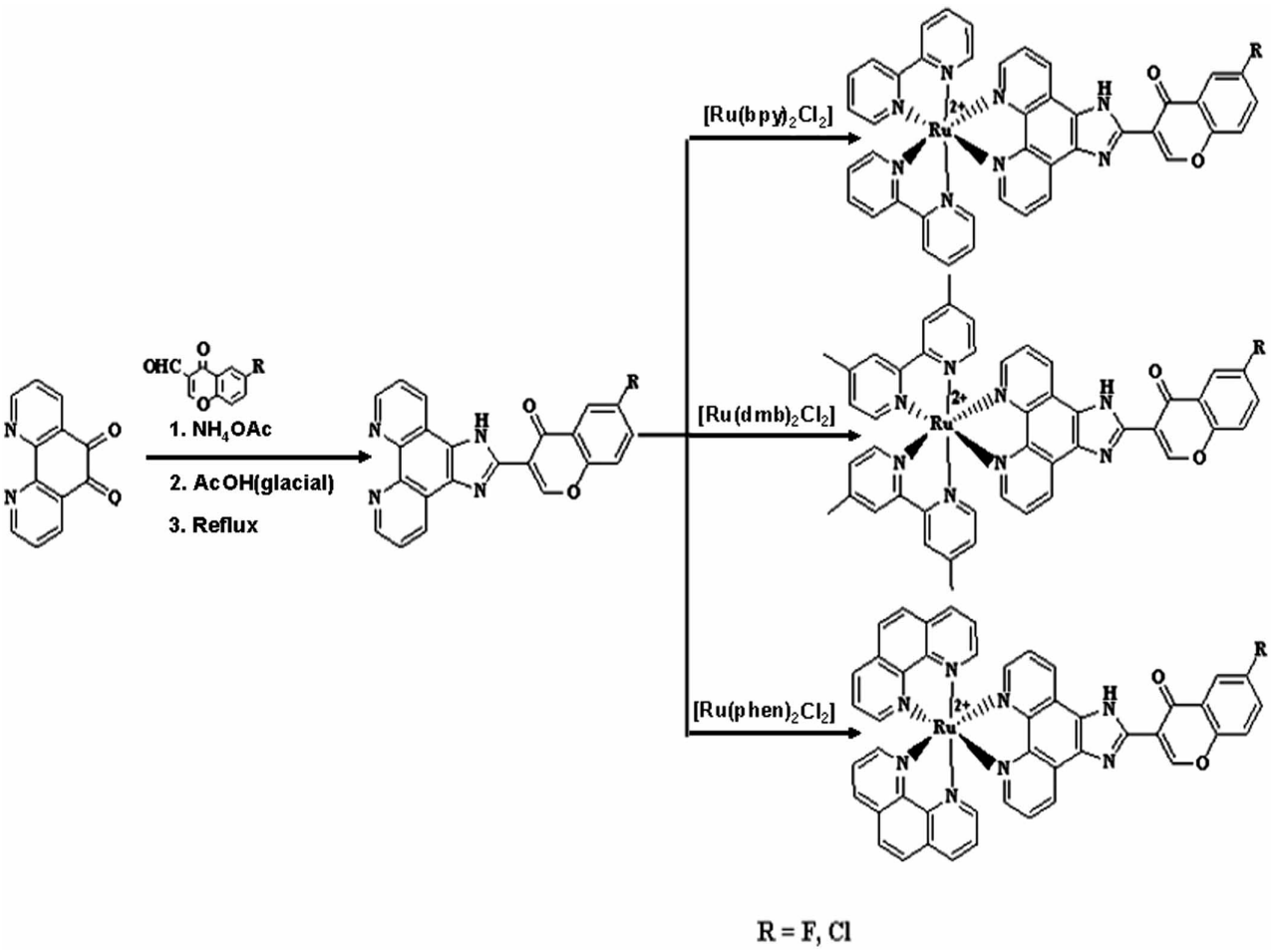

Scheme 1. Synthetic routines of ligands and Ru(II) complexes.

Table 1. Elemental analysis data.

Compound	Elemental analysis; found (calcd)
FIPC	C:69.0(69.1); H:2.75(2.90); N:14.6(14.6)
ClIPC	C:66.2(66.3); H:2.5(2.8); N:14.0(14.05)
$[Ru(bipy)_2(FIPC)]^{2+}$	C:44.78(44.96); H:2.65(2.76); N:9.62(9.99)
$[Ru(dmb)_2(FIPC)]^{2+}$	C:46.85(46.90); H:3.25(3.31); N:9.25(9.51)
$[Ru(phen)_2(FIPC)]^{2+}$	C:47.11(47.22); H:2.58(2.65); N:9.40(9.58)
$[Ru(bipy)_2(ClIPC)]^{2+}$	C:44.28(44.30); H:2.64(2.72); N:9.74(9.84)
$[Ru(dmb)_2(ClIPC)]^{2+}$	C:46.21(46.25); H:3.15(3.26); N:9.20(9.38)
$[Ru(phen)_2(ClIPC)]^{2+}$	C:46.51(46.56); H:2.58(2.61); N:9.45(9.44)

(0.260 g, 1.2 mmol), 6-chloro-4-oxo-4H-chromene-3-carbaldehyde (0.374 g, 1.8 mmol) in ammonium acetate (1.9 g, 25 mmol) and glacial acetic acid (10 ml) by refluxing for 2 h. The deep red solution obtained was cooled, diluted with water (25 cm^3) and neutralised with ammonia. Then, the mixture was filtered and the precipitates were washed with H_2O and Me_2CO, and then dried (yield: 86%).

Synthesis of [Ru(bipy)$_2$ (FIPC)] (PF$_6$)$_2$·2H$_2$O

$[Ru(bipy)_2FIPC]^{2+}$ was synthesised using a mixture of *cis*-$[Ru(bipy)_2Cl_2]$ $2H_2O$ (0.104 g, 0.2 mmol), FIPC (0.076 g, 0.2 mmol) and ethanol (70 ml), and the mixture was refluxed under nitrogen for 2 h. Upon cooling, the resulting clear solution was filtered. The filtrate was treated with a saturated aqueous solution of ammonium hexafluorophosphate, and a red precipitate was obtained (yield: 85%).

Synthesis of [Ru(dmb)$_2$ (FIPC)] (PF$_6$)$_2$· 2H$_2$O

This complex was obtained by a similar procedure to that described above, *cis*-$[Ru(dmb)_2Cl_2]$ $2H_2O$ (0.116 g, 0.2 mmol) in the place of *cis*-$[Ru(bipy)_2Cl_2]$ $2H_2O$ (yield: 82%).

Synthesis of [Ru(phen)$_2$ (FIPC)] (PF$_6$)$_2$· 2H$_2$O

This complex was obtained by a similar procedure to that described above, *cis*-$[Ru(phen)_2Cl_2]$ $2H_2O$ (0.114 g, 0.2 mmol) in the place of *cis*-$[Ru(bipy)_2Cl_2]$ $2H_2O$ (yield: 88%).

Synthesis of [Ru(bipy)$_2$ (ClIPC)] (PF$_6$)$_2$· 2H$_2$O

$[Ru(bipy)_2ClIPC]^{2+}$ was synthesised using a mixture of *cis*-$[Ru(bipy)_2Cl_2]$ $2H_2O$ (0.104 g, 0.2 mmol), ClIPC (0.079 g, 0.2 mmol) and ethanol (70 ml), and the mixture was refluxed under nitrogen for 2 h. Upon cooling, the resulting clear solution was filtered. The filtrate was treated with a saturated aqueous solution of ammonium hexafluorophosphate, and a red precipitate was obtained (yield: 86%).

Synthesis of [Ru(dmb)$_2$ (ClIPC)] (PF$_6$)$_2$· 2H$_2$O

This complex was obtained by a similar procedure to that described above, *cis*-$[Ru(dmb)_2Cl_2]$ $2H_2O$ (0.116 g, 0.2 mmol) in place of *cis*-$[Ru(bipy)_2Cl_2]$ $2H_2O$ (yield: 79%).

Synthesis of [Ru(phen)$_2$ (ClIPC)] (PF$_6$)$_2$· 2H$_2$O

This complex was obtained by a similar procedure to that described above, *cis*-[Ru (phen)$_2$Cl$_2$] $2H_2O$ (0.114 g, 0.2 mmol) in place of *cis*-$[Ru(bipy)_2Cl_2]$ $2H_2O$ (yield: 85%).

For all the complexes synthesised above, ^1H, $^{13}C[^1H]$ NMR, IR and elemental analysis data are given in Tables 1–4.

Table 2. IR data.

Compound	IR data (cm^{-1})
FIPC	1615(C═O), 1556(C═N), 1434(C═C)
ClIPC	1610(C═O), 1526(C═N), 1412(C═C)
$[Ru(bipy)_2(FIPC)]^{2+}$	1645(C═O), 1578(C═N), 1474(C═C), 624(Ru-N(FIPC)), 585(Ru-N(bipy))
$[Ru(dmb)_2(FIPC)]^{2+}$	1642(C═O), 1570(C═N), 1462(C═C), 624(Ru-N(FIPC)), 581(Ru-N(dmb))
$[Ru(phen)_2(FIPC)]^{2+}$	1654(C═O), 1585(C═N), 1484(C═C), 627(Ru-N(FIPC)), 581(Ru-N(phen))
$[Ru(bipy)_2(ClIPC)]^{2+}$	1616(C═O), 1564(C═N), 1464(C═C), 626(Ru-N(ClIPC)), 580(Ru-N(bipy))
$[Ru(dmb)_2(ClIPC)]^{2+}$	1640(C═O), 1571(C═N), 1462(C═C), 625(Ru-N(ClIPC)), 582(Ru-N(dmb))
$[Ru(phen)_2(ClIPC)]^{2+}$	1632(C═O), 1578(C═N), 1477(C═C), 626(Ru-N(ClIPC)), 584(Ru-N(phen))

Table 3. ^{1}H NMR data.

Compound	^{1}H NMR data (δ, ppm)
FIPC	9.05 (s, 2H, H_a, $H_{a'}$), 8.80–8.70 (d, 2H, H_c, $H_{c'}$), 7.80 (s, 2H, H_o), 7.55 (s, 2H, H_k), 7.47–7.36 (d, 2H, H_q), 7.30 (s, 2H, H_b $H_{b'}$), 7.15 (d,1H, H_r)
ClIPC	8.95 (s, 2H, H_a, $H_{a'}$), 8.65 (s, 2H, H_c, $H_{c'}$), 7.80–7.60 (d, 2H, H_o), 7.38 (s, 2H, H_k), 7.37–7.26 (d, 2H, H_q), 7.25–7.18 (s, 2H, H_b), 7.00–6.86 (d,1H, H_r)
$[Ru(bipy)_2(FIPC)]^{2+}$	9.68–9.58 (d, 2H, H_a, $H_{a'}$), 9.38 (s, 4H, H_1, $H_{1'}$), 9.15–9.05 (d, 4H, H_4, $H_{4'}$), 8.90–8.78 (m, 2H, H_c, $H_{c'}$), 8.23–8.07 (t, 4H, H_3, $H_{3'}$), 8.15–8.00 (m, 2H, H_k, H_o), 7.98–7.92 (m, 2H, H_b, $H_{b'}$), 7.90–7.80 (d, 4H, H_2, $H_{2'}$), 7.65–7.55 (t, 1H, H_q), 7.38–7.28 (t, 1H, H_r)
$[Ru(dmb)2(FIPC)]^{2+}$	9.36–9.30 (d, 2H, H_a, $H_{a'}$), 9.13–9.06 (d, 4H, H_1, $H_{1'}$), 8.82–8.70 (d, 4H, H_4, $H_{4'}$), 8.42–8.36 (t, 2H, H_c, $H_{c'}$), 8.15–8.10 (t, 1H, H_k), 8.08–8.05 (d, 1H, H_o), 8.04–7.96 (m, 2H, H_b, $H_{b'}$), 7.83–7.70 (m, 4H, H_2, $H_{2'}$), 7.32–7.24 (d, 1H, H_q), 7.21–7.17 (d, 1H, H_r), 2.88 (s, 6H, H_6), 2.73 (s, 6H, $H_{6'}$)
$[Ru(phen)_2(FIPC)]^{2+}$	9.60 (s, 2H, H_a, $H_{a'}$), 9.50–9.43 (d, 4H, H_1, $H_{1'}$), 9.39 (s, 2H, H_c, $H_{c'}$), 9.32–9.21 (t, 4H, H_3, $H_{3'}$), 9.10–8.98 (d, 4H, C_6, $C_{6'}$). 8.81–8.73 (d, 1H, H_k), 8.43–8.34 (d, 1H, H_o), 8.15–8.05 (d, 4H, H_b, $H_{b'}$), 8.05–7.92 (m, 2H, H_2, $H_{2'}$), 7.85–7.70 (m, 2H, H_q, H_r)
$[Ru(bipy)_2(ClIPC)]^{2+}$	9.75–9.68 (d, 2H, H_a, $H_{a'}$), 9.35–9.25 (d, 4H, H_1, $H_{1'}$), 9.20–9.10 (d, 4H, H_4, $H_{4'}$), 9.10–9.00 (d, 2H, H_c, $H_{c'}$), 8.78–8.65 (d, 4H, H_3, $H_{3'}$), 8.05–8.00 (t, 1H, H_o), 7.90–7.80 (m, 1H, H_k), 7.70–7.60 (m, 1H, H_q), 7.42–7.38 (d, 2H, H_b, $H_{b'}$), 7.34 (s, 4H, H_2, $H_{2'}$), 7.05–7.00 (d, 1H, H_r)
$[Ru(dmb)_2(ClIPC)]^{2+}$	9.40 (s, 2H, H_a, $H_{a'}$), 8.80–8.64 (d, 4H, H_1, $H_{1'}$), 8.27–8.23 (d, 4H, H_4, $H_{4'}$), 8.12 (s, 2H, H_c, $H_{c'}$), 8.05–8.03 (d, 1H, H_o), 8.03–7.99 (t, 1H, H_k), 7.97–7.90 (t, 1H, H_q), 7.74–7.66 (d, 2H, H_b, $H_{b'}$), 7.51–7.37 (d, 4H, H_2, $H_{2'}$), 7.25–7.14 (d, 1H, H_r), 2.60 (s, 6H, H_6), 2.57 (s, 6H, $H_{6'}$)
$[Ru(phen)_2(ClIPC)]^{2+}$	9.24 (s, 2H, H_a, $H_{a'}$), 9.08–9.00 (d, 4H, H_1, $H_{1'}$), 8.75–8.70 (t, 2H, H_c, $H_{c'}$), 8.60–8.50 (d, 4H, H_3, $H_{3'}$), 8.24–8.15 (d, 1H, H_o), 8.12–8.08 (d, 4H, C_6, $C_{6'}$), 7.93 (s, 1H, H_k), 7.89 (s, 1H, H_q), 7.79–7.68 (t, 2H, H_b, $H_{b'}$), 7.68–7.60 (m, 4H, H_2, $H_{2'}$), 7.56–7.48 (t, 1H, H_r)

Physical measurements

UV–vis spectra were recorded with an Elico Bio-spectra-photometer, model BL198. IR spectra were recorded in KBr discs on a Perkin-Elmer FT-IR-1605 spectrometer. ^{1}H and ^{13}C[^{1}H] NMR spectra were measured on a Varian XL-300 MHz spectrometer using DMSO-d_6 as solvent and TMS as an internal standard. Microanalyses (C, H and N) were carried out on a Perkin-Elmer 240 elemental analyzer. Fluorescence spectra were recorded with a JASCO Model 7700 spectrofluorometer for solutions

Table 4. ^{13}C [^{1}H] NMR data.

Compound	^{13}C [^{1}H] NMR (DMSO d_6, δ, ppm)
$[Ru(bipy)_2(FIPC)]^{2+}$	172.00 (1C, C_l), 153.80 (1C, C_k), 151.42 (5C, C_p, C_5, $C_{5'}$), 150.60 (2C, C_e, $C_{e'}$), 147.70 (1C, C_n), 145.72 (6C, C_1, $C_{1'}$, C_a, $C_{a'}$), 137.30 (1C, C_i), 136.16 (6C, C_c, $C_{c'}$, C_3, $C_{3'}$), 131.00 (2C, C_d, $C_{d'}$), 128.53 (1C, C_m), 127.40 (5C, C_f, C_4, $C_{4'}$), 126.80 (1C, C_g), 126.00 (1C, C_q), 121.78 (2C, C_b, $C_{b'}$), 119.10 (4C, C_2, $C_{2'}$), 117.50 (1C, C_r). 115.60 (1C, C_j), 113.90 (1C, C_o)
$[Ru(dmb)_2(FIPC)]^{2+}$	173.60 (1C, C_l), 158.60 (4C, C_5, $C_{5'}$), 157.80 (2C, C_k, C_p), 156.50 (2C, C_e, $C_{e'}$), 153.30 (1C, C_n), 152.70 (6C, C_1, $C_{1'}$, C_a, $C_{a'}$), 152.10 (4C, C_3, $C_{3'}$), 150.60 (1C, C_i)), 147.20 (4C, C_c, $C_{c'}$, C_d, $C_{d'}$), 145.90 (1C, C_m), 136.80 (4C, C_2, $C_{2'}$), 136.70 (4C, C_4, $C_{4'}$), 130.40 (1C, C_f), 128.00 (1C, C_g), 126.30 (1C, C_q), 121.70 (2C, C_b, $C_{b'}$), 114.00 (1C, C_r), 110.00 (1C, C_j), 109.70 (1C, C_o), 30.70 (4C, C_6, $C_{6'}$)
$[Ru(phen)_2(FIPC)]^{2+}$	174.30 (1C, C_l), 152.90 (2C, C_k, C_p), 152.40 (2C, C_e, $C_{e'}$), 150.60 (1C, C_n), 149.80 (6C, C_1, $C_{1'}$, C_a, $C_{a'}$), 146.90 (1C, C_i), 136.50 (4C, C_5, $C_{5'}$), 130.10 (6C, C_c, $C_{c'}$, C_3, $C_{3'}$), 127.70 (4C, C_4, $C_{4'}$), 126.00 (4C, C_6, $C_{6'}$). 125.50 (2C, C_d, $C_{d'}$), 121.00 (1C, C_m), 118.30 (2C, C_f, C_g), 116.80 (1C, C_q), 114.80 (6C, C_2, $C_{2'}$, C_b, $C_{b'}$), 113.20 (2C, C_r, C_j), 106.00 (1C, C_o)
$[Ru(bipy)_2(ClIPC)]^{2+}$	176.00 (1C, C_l), 158.80 (1C, C_k), 157.00 (4C, C_5, $C_{5'}$), 154.00 (1C, C_n), 152.00 (6C, C_1, $C_{1'}$, C_a, $C_{a'}$), 150.00 (2C, C_e, $C_{e'}$), 146.00 (1C, C_i), 138.00 (6C, C_c, $C_{c'}$, C_3, $C_{3'}$), 134.80 (1C, C_q), 131.00 (2C, C_o, C_p), 128.00 (6C, C_2, $C_{2'}$, C_b, $C_{b'}$), 126.20 (2C, C_d, $C_{d'}$), 124.60 (5C, C_f, C_4, $C_{4'}$), 124.00 (1C, C_m), 121.80 (1C, C_g), 114.40 (2C, C_r, C_j)
$[Ru(dmb)_2(ClIPC)]^{2+}$	173.00 (1C, C_l), 159.00 (1C, C_k), 156.00 (4C, C_5, $C_{5'}$), 154.00 (3C, C_n, C_e, $C_{e'}$), 151.00 (6C, C_1, $C_{1'}$, C_a, $C_{a'}$), 150.00 (4C, C_3, $C_{3'}$), 146.00 (1C, C_i), 138.80 (2C, C_c, $C_{c'}$), 135.00 (1C, C_q), 131.00 (2C, C_o, C_p), 128.80 (2C, C_d, $C_{d'}$), 125.00 (4C, C_4, $C_{4'}$), 124.50 (1C, C_m), 124.00 (1C, C_f, C_g), 121.40 (6C, C_2, $C_{2'}$, C_b, $C_{b'}$), 114.40 (2C, C_r, C_j). 21.00 (4C, C_6, $C_{6'}$)
$[Ru(phen)_2(ClIPC)]^{2+}$	177.00 (1C, C_l), 160.00 (1C, C_k), 158.00 (1C, C_n), 154.50 (3C, C_e, $C_{e'}$), 154.00 (6C, C_1, $C_{1'}$, C_a, $C_{a'}$), 147.00 (4C, C_5, $C_{5'}$), 144.00 (1C, C_i), 137.00 (6C, C_3, $C_{3'}$, C_c, $C_{c'}$), 135.00 (1C, C_q), 133.00 (1C, C_o), 131.00 (4C, C_4, $C_{4'}$), 129.00 (1C, C_p), 128.00 (4C, C_6, $C_{6'}$), 126.50 (6C, C_2, $C_{2'}$, C_b, $C_{b'}$), 126.00 (2C, C_d, $C_{d'}$), 125.00 (1C, C_m), 124.00 (1C, C_f), 121.00 (1C, C_g), 115.00 (2C, C_r, C_j)

having absorbance less than 0.2 at the excitation wavelength. Viscosity experiments were carried out on the Ostwald viscometer, immersed in thermostated water bath maintained at 30 ± 0.1°C. CT-DNA samples approximately 200 bp in average length were prepared by sonication in order to minimise complexities arising from DNA flexibility (*33*). Data were presented as $(\eta/\eta_0)^{1/3}$ vs. concentration of [Ru(II)]/[DNA], where η is viscosity of DNA in the presence of the complex, and η_0 is the viscosity of DNA alone. Viscosity values were calculated from the observed flow time of DNA-containing solutions ($t > 100$ s) corrected for the flow time of buffer alone (t_0) (*12*). The DNA-melting experiments were carried out by controlling the temperature of the sample cell with a Shimadzu circulating bath while monitoring the absorbance at 260 nm. For the gel electrophoresis experiments, the super coiled pBR-322 DNA (100 μM) was treated with Ru(II) complexes in 50 mM Tris–HCl, 18 mM NaCl buffer, pH 7.8, and the solutions were then irradiated for 2 h at room temperature with a UV lamp (365 nm, 10 W). The samples were analysed by electrophoresis for 2.5 h at 40 V on a 1% agarose gel in Tris–acetic acid–EDTA buffer, pH 7.2. The gel was stained with 1 μg/ml ethidium bromide (EtBr) and photographed under UV light.

The antimicrobial tests were performed by the standard disc diffusion method (*34*). The complexes were screened for their antifungal activity against the fungi viz. *Aspergillus niger*. These fungal species were isolated from the infected parts of the host plants on *M* test agar medium. The cultures of the fungi were purified by single-spore isolation technique. A concentration of 1.5 mg/ml of each Ru(II) complex compound in DMSO solution was prepared for testing against the spore germination of each fungus. Filter paper discs of 5 mm size were prepared by using Whatman filter paper no. 1 (sterilised in an autoclave) and that was saturated with 10 μl of the Ru(II) complex compounds dissolved in DMSO solution or DMSO as the negative control. The fungal culture plates were inoculated and incubated at 25 ± 0.2°C for 48 h. The plates were then observed, and the diameters of the inhibition zones (in mm) were measured and tabulated. The results were also compared with a standard antifungal drug flucanazole at the same concentration.

The antibacterial activity of the complexes was studied against four human pathogenic bacteria, *Bacillus subtilis* (G^+), *Escherichia coli* (G^-), *Staphylococcus aureus* (G^+) and *Klebsiella pneumoniae* (G^-). Each of the Ru(II) complex compounds solution was prepared by dissolving in DMSO at a concentration of 1 mg/ml. Paper discs of Whatman filter paper no. 1 were cut and sterilised in an autoclave. The paper discs were saturated with 10 μl of the Ru(II) complex compounds dissolved in DMSO solution or DMSO as the negative control and were placed aseptically in the Petri dishes containing *M* test agar media inoculated with *B. subtilis*, *S. aureus*, *E. coli* and *K. pneumoniae* bacteria separately. The Petri dishes were incubated at 37°C, and the inhibition zones were recorded after 24 h of incubation. The results were also compared with a standard antibacterial drug streptomycin at the same concentration. The filter paper discs of 4 mm size were prepared (Whatman filter paper no. 42).

Results and discussion

Spectral characterisation

All the compounds synthesised in this study have been characterised by elemental analysis, UV–vis, IR, ^{1}H and ^{13}C[^{1}H] NMR spectroscopic methods. Electronic absorption spectra of the complexes are characterised by metal to ligand charge transfer (MLCT) transition in the visible region. The low energy bands at region 446 nm for complex 1, 451 nm for complex 2, 446 nm for complex 3, 446 nm for complex 4, 453.5 nm for complex 5 and 438.5 nm for complex 6 are assigned to MLCT transition. In the ^{1}H NMR spectra of the six Ru(II) complexes (1–6), the peaks due to various protons of bipy, phen, dmb, FIPC and ClIPC are seen to be shifted in comparison with the corresponding free ligands suggesting complexation. All the relative chemical shifts of carbons of Ru(II) complexes are shifted downfield. The ^{1}H and ^{13}C [^{1}H] NMR spectra of the Ru(II) complexes have been recorded in DMSO-d_6. In ^{13}C NMR, the characteristic peak of FIPC and ClIPC (C═O) appears at 172.5, 173.0. Whereas in $[Ru(bipy)_2FIPC]^{2+}$(1), $[Ru(dmb)_2FIPC]^{2+}$(2), $[Ru(phen)_2FIPC]^{2+}$(3), $[Ru(bipy)_2ClIPC]^{2+}$(4), $[Ru(dmb)_2ClIPC]^{2+}$(5) and $[Ru(phen)_2ClIPC]^{2+}$(6) complexes, (C═O) carbon shifts downfield. The ^{1}H and ^{13}C NMR spectra of the $[Ru(bipy)_2FIPC]^{2+}$ and $[Ru(dmb)_2ClIPC]^{2+}$ complexes are shown in Figures 1 and 2.

DNA-binding studies

Absorption spectral studies

The binding of intercalative ligand to DNA has been characterised classically through absorption titration. Absorption titrations of Ru(II) complexes were done using a fixed ruthenium concentration to which increments of the DNA stock solution were added. The absorption spectra of complexes in the absence and presence of CT-DNA are given in Figure 3. The absorption spectra of complexes are characterised by distinct intense MLCT transitions in the vis region, which are attributed to Ru ($d\pi$) → bipy (π^*), dmb (π^*), phen (π^*) and Ru ($d\pi$) → FIPC (π^*), Ru ($d\pi$) → ClIPC (π^*) transitions, the bonds between 290 and 300 nm for complexes 1–6 are attributed to intraligand $\pi \rightarrow \pi^*$ transitions and MLCT in lower energy region around 450 nm. As the concentration of

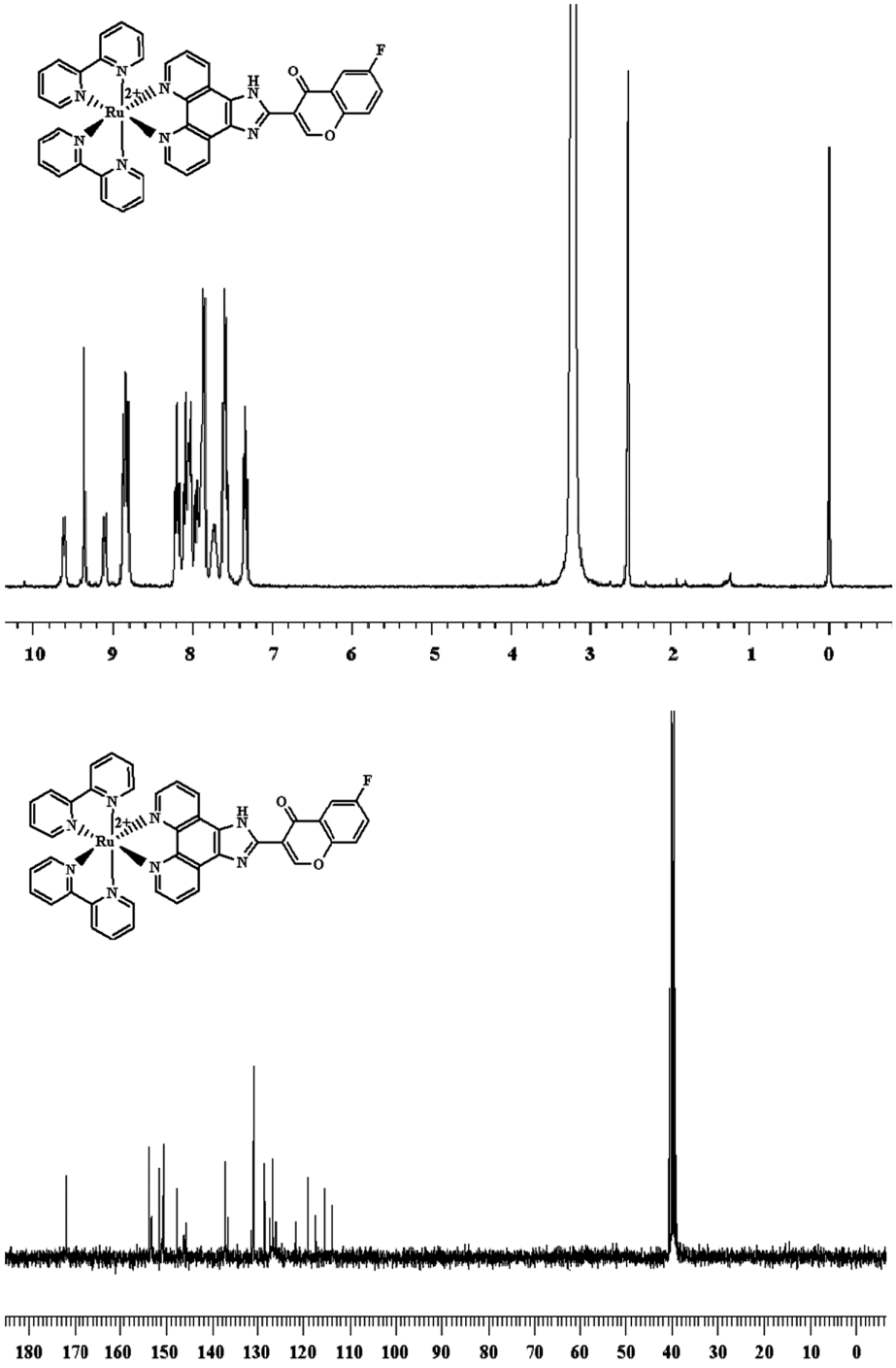

Figure 1. ^{1}H and ^{13}C [^{1}H] NMR spectra of $[Ru(bipy)_2\ FIPC]^{2+}$ in DMSO-d_6.

DNA is increased, the hypochromism in the MLCT band increases although obvious red shift is observed. In the absorption spectra, the extent of spectral changes closely correlates with the DNA-binding affinities of the complexes. Due to the intercalative mode involving a stacking interaction between an aromatic chromophore and the base pair of DNA, the extent of the hypochromism commonly parallels the intercalative binding strength. Addition of increasing amounts of CT-DNA results in decrease in the peak intensities in the UV spectra of Ru(II) complexes 1–6, suggesting a mode of binding involving a stacking interaction between the complex and the base pairs of DNA. The spectral shifts for intercalation mode are usually greater than those in a groove-binding mode.

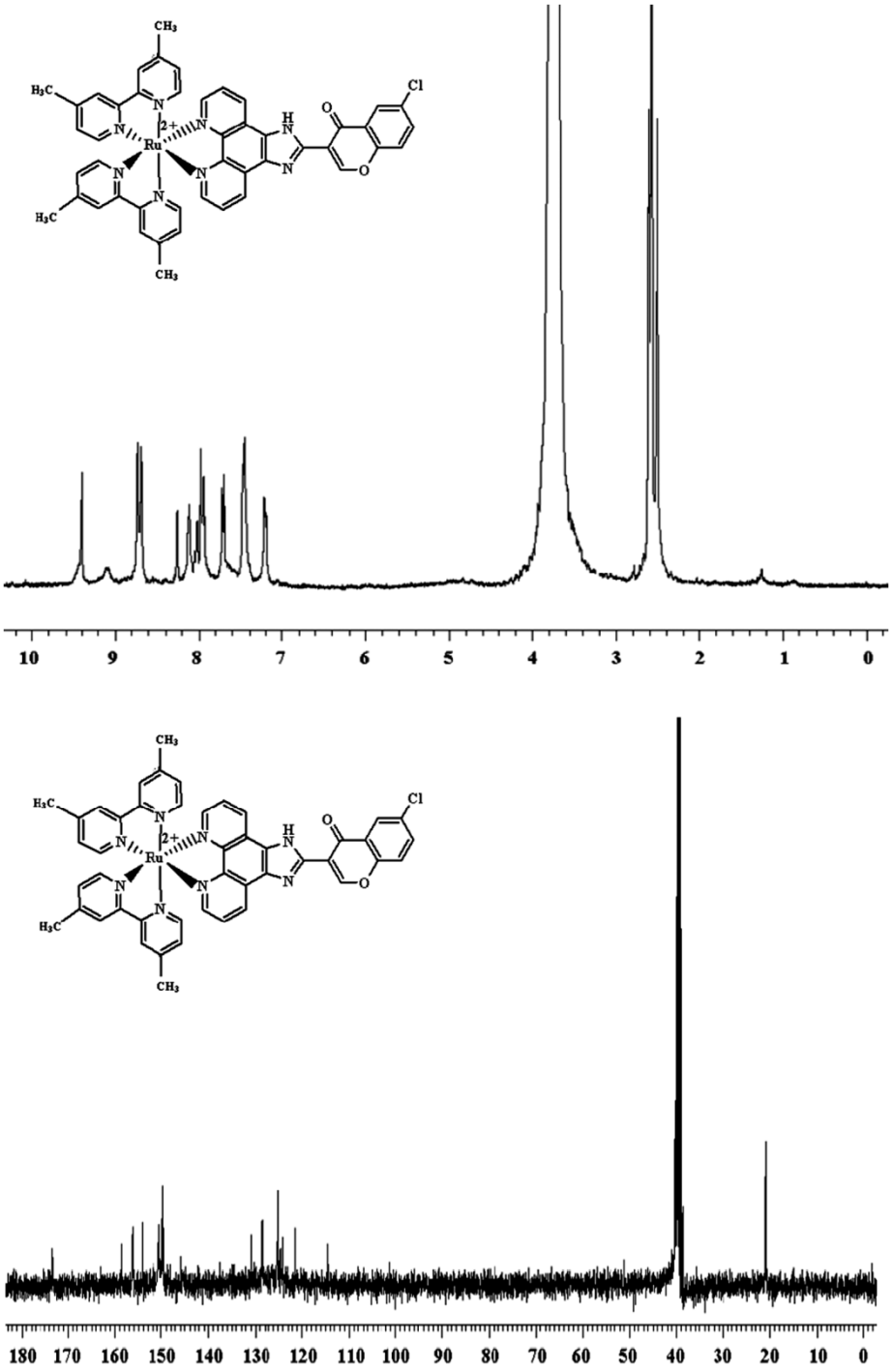

Figure 2. ^{1}H and ^{13}C [^{1}H] NMR spectra of $[Ru(dmb)_2\ ClIPC]^{2+}$ in DMSO-d_6.

As the concentration increased, the MLCT bands of the complexes 1–6 exhibited hypochromism about 12.5, 9.2, 14.6, 10.6, 9.0 and 12.8% as well as insignificant bathochromism about 8.0, 5.0, 12.5, 7.5, 5.0 and 10.0 nm, respectively. These results are similar to those reported earlier for various metallo-intercalators (*35*, *36*). Based on the observations, we assume that there are some interactions between the complexes and the base pairs of DNA. To compare quantitatively the affinity of the complexes towards DNA, the intrinsic binding constants K of the Ru(II) complexes to CT-DNA were determined by monitoring the change of absorbance at λ_{max} of the

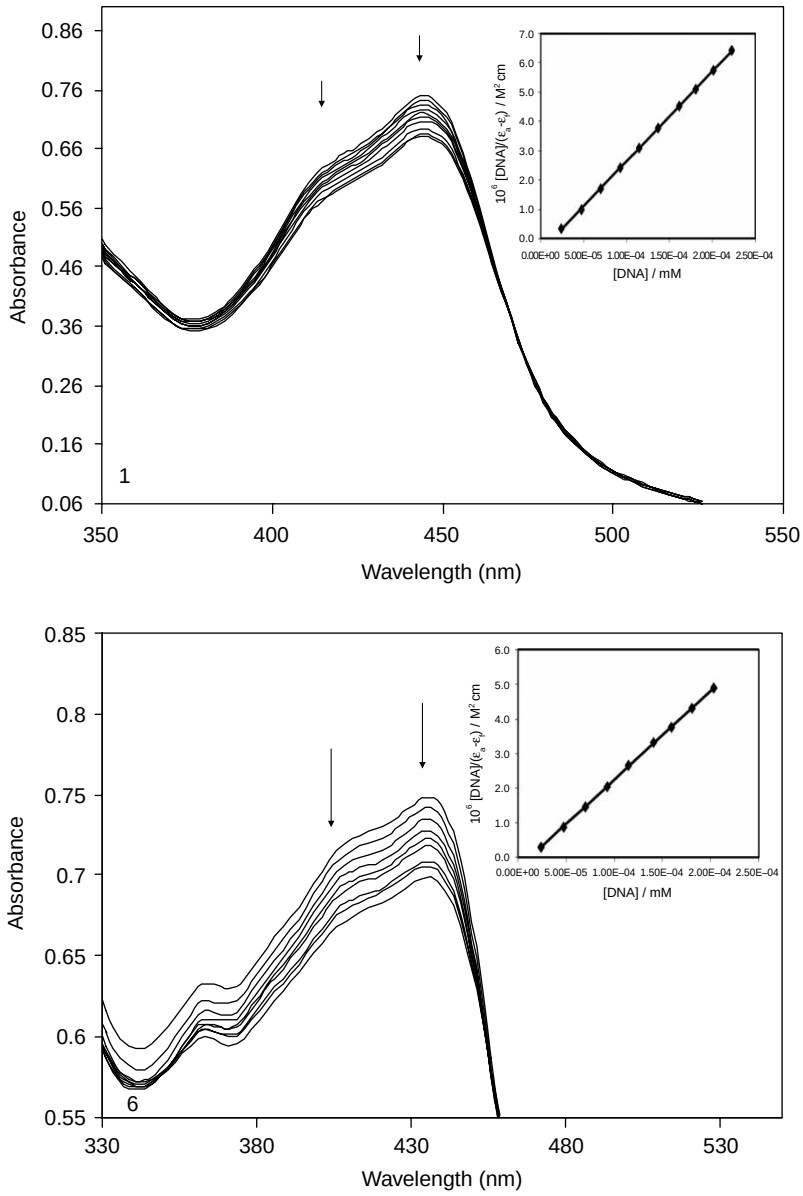

Figure 3. Absorption spectra of complexes $[Ru(bipy)_2FIPC]^{2+}$(1) and $[Ru(phen)_2ClIPC]^{2+}$(6) in Tris–HCl buffer at 25°C in the presence of increasing amount of CT-DNA, [Ru] = 20 μM, [DNA] = 0–120 μM. The arrows indicate the change in absorbance upon increasing the DNA concentration. Inset: Plot of [DNA]/($\varepsilon_a - \varepsilon_f$) vs. [DNA] for titration of the Ru(II) complexes.

complex in the visible region, with increasing concentration of DNA (*37*). The intrinsic binding constants K of the complexes with CT-DNA were determined according to following equation (*38*) through a plot of [DNA]/($\varepsilon_a - \varepsilon_f$) vs. [DNA].

$$\frac{[DNA]}{\varepsilon_a - \varepsilon_f} = \frac{[DNA]}{\varepsilon_b - \varepsilon_f} + \frac{1}{K_b(\varepsilon_b - \varepsilon_f)},$$

where [DNA] is the concentration per nucleotide. The apparent absorption coefficient ε_a, ε_f and ε_b, correspond to A_{obs}/Ru(II), ε_a extinction coefficients for the free Ru(II) complex, ε_f extinction coefficient of the complex in presence of DNA and ε_b the extinction coefficients for the Ru(II) complex in the fully bound form, respectively. In plots of [DNA]/($\varepsilon_a - \varepsilon_f$) vs. [DNA], K_b is given by the ratio of slope to intercept. Intrinsic binding constants, K_b of complexes 1–6, are $7.5 \pm 0.1 \times 10^4$, $5.9 \pm 0.1 \times 10^4$, $9.0 \pm 0.1 \times 10^4$, $6.8 \pm 0.1 \times 10^4$, $5.5 \pm 0.1 \times 10^4$ and $8.6 \pm 0.1 \times 10^4\,M^{-1}$, respectively and follow the order $3 > 6 > 1 > 4 > 2 > 5$. These K_b values are smaller than those of classical intercalators, such as $[Ru(bipy)_2(dppz)]^{2+}$($>10^6$) (*13*), $[Ru(bipy)_2(ppd)]^{2+}$ ($K = 1.3 \times 10^6$) (*39*) and comparable to those of $[Ru(bipy)_2(MCMIP)]^{2+}$

(3.92×10^4), $[Ru(phen)_2(MCMIP)]^{2+}(4.8 \times 10^4)$ (*40*), $[Ru(dmb)_2(MCMIP)]^{2+}(2.25 \times 10^4)$ and $[Ru(dmp)_2(MCMIP)]^{2+}(5.42 \times 10^4)$ (*41*). The difference between the binding constants of the two series (1, 2, 3 and 4, 5, 6) is due to different ancillary ligands and different functional groups on the polypyridyl ligand. In this, fluoro polypyridyl Ru(II)complexes (1, 2, 3) bind more effectively to CT-DNA than to chloro polypyridyl Ru(II) complexes (4, 5, 6). Fluoro is more electron withdrawing than chloro, hence makes the ring more electron deficient than chloro substituted ring. Electron deficient rings interact more strongly with polyanion (DNA) than electron rich rings. Complexes 2 and 5 show the least binding strength to double-helical DNA. Due to the presence of methyl groups on the 4- and 4′- positions of the ancillary ligand, dmb causes steric hindrance when the complex intercalates into the DNA base pairs, hence decreasing the binding constant.

Fluorescence spectroscopic studies

The emission intensities of complexes from their MLCT excited state are found to depend on the DNA concentration. The emission spectra of the complexes 1–6 in the absence and the presence of CT-DNA are shown in Figure 4. In the absence of DNA and at 423 nm excitation, these six complexes emit relatively moderate luminescence in Tris buffer at room temperature with the emission maxima at 598–600 nm, respectively. The change in emission may arise from the interannular twisting between phen and other substituents. Here, the introduction of 6-fluoro-4-oxo-4 H-chromene to the FIPC and 6-chloro-4-oxo-4 H-chromene to the ClIPC ligands may be responsible for the negligible luminescence. The luminescent properties of the complexes were perturbed when DNA was added to the complex solution, and binding of the complexes to DNA was found to increase the fluorescence intensity. Upon addition of CT-DNA, the emission enhances 3.80, 3.40, 4.20, 3.50, 3.20 and 4.00 times for complexes 1–6, than the complex without DNA, respectively. The intrinsic binding constant of fluorescence was obtained from a modified Scatchard equation (*42*), through a plot of r/C_f vs. r, where r is the C_b/[DNA] and C_f is the concentration of the free metal complex. C_b is obtained from $C_b = C_t[(F - F_0)/(F_{max} - F_0)]$, where C_t is the total complex concentration, F is the observed fluorescence emission intensity at a given DNA concentration, F_0 is the intensity in the absence of DNA and F_{max} is the fully bound DNA to complex, the binding constant is given by the ratio of slope to intercept. Scatchard plots for complexes have been constructed from luminescence spectra, and binding constants were $8.5 \pm 0.1 \times 10^4$, $6.1 \pm 0.1 \times 10^4$, $9.2 \pm 0.1 \times 10^4$, $7.2 \pm 0.1 \times 10^4$, $5.8 \pm 0.1 \times 10^4$ and $8.8 \pm 0.1 \times 10^4\,M^{-1}$, respectively. The different K_b values obtained by the two titration methods of measurements (absorption and fluorescence titration), as recently suggested by Wu et al. (*43*), are in good agreement with that of absorption spectroscopy.

A highly negatively charged quencher is expected to be repelled by the negatively charged phosphate back bone, and therefore a DNA-bound cationic complex should be less quenched by anionic quencher, than the unbound complex (*44*). $[Fe(CN)_6]^{4-}$ quencher is used to observe the binding of complexes 1–6 with CT-DNA. As illustrated in Figure 5, in the absence of DNA, the Ru(II) complex is efficiently quenched by $[Fe(CN)_6]^{4-}$, whereas the complex bound to DNA was protected from the quencher. From quenching studies, it is clear that DNA-binding ability of complexes follows the order: $3 > 6 > 1 > 4 > 2 > 5$.

Steady-state emission quenching experiments using $[Fe(CN)_6]^{4-}$ as quencher are also used to observe the binding of Ruthenium(II) complexes with CT-DNA. The Stern–Volmer quenching constant (K_{sv}) can be determined by using the Stern–Volmer equation (*45*)

$$\frac{I_0}{I} = 1 + K_{sv}[Q],$$

where I_0 and I are the intensities of the fluorophore in the absence and presence of quencher, respectively, Q is the concentration of the quencher and K_{sv} is a linear Stern–Volmer quenching constant. Figure 5 shows the Stern–Volmer plots for the free complex in solution and in the presence of increasing amount of DNA. All the complexes show linear Stern–Volmer plots. The K_{sv} value for the complexes in the absence of DNA for complexes 1–6 is 106, 102, 130, 104, 98 and 124, respectively.

The K_{sv} value for the six complexes in the presence of DNA is 82, 74, 100, 78, 70 and 98. In the presence of DNA, the K_{sv} value is smaller and at high concentration of DNA (1:200; Ru^{2+}:DNA) essentially zero slope, indicating that the bound complex is inaccessible to the quencher.

Viscosity studies

The DNA-binding modes of complexes were further investigated by viscosity measurement. The viscosity measurements of DNA are regarded as the least ambiguous and the critical test of a DNA-binding model in solution and provide strong evidence for intercalative DNA-binding mode (*12*, *46*). A classical intercalation model results in lengthening the DNA helix, as base pairs are separated to accommodate the binding ligand, leading to the increase of DNA viscosity. In contrast, a partial non-classical intercalation of the ligand could bend (or kink) the DNA helix, and reduce its effective length (*12*, *47*). For example, under appropriate conditions, intercalation of dye-like EtBr causes a significant increase in the over all DNA length. The effects of the six complexes on the viscosity of rod-like

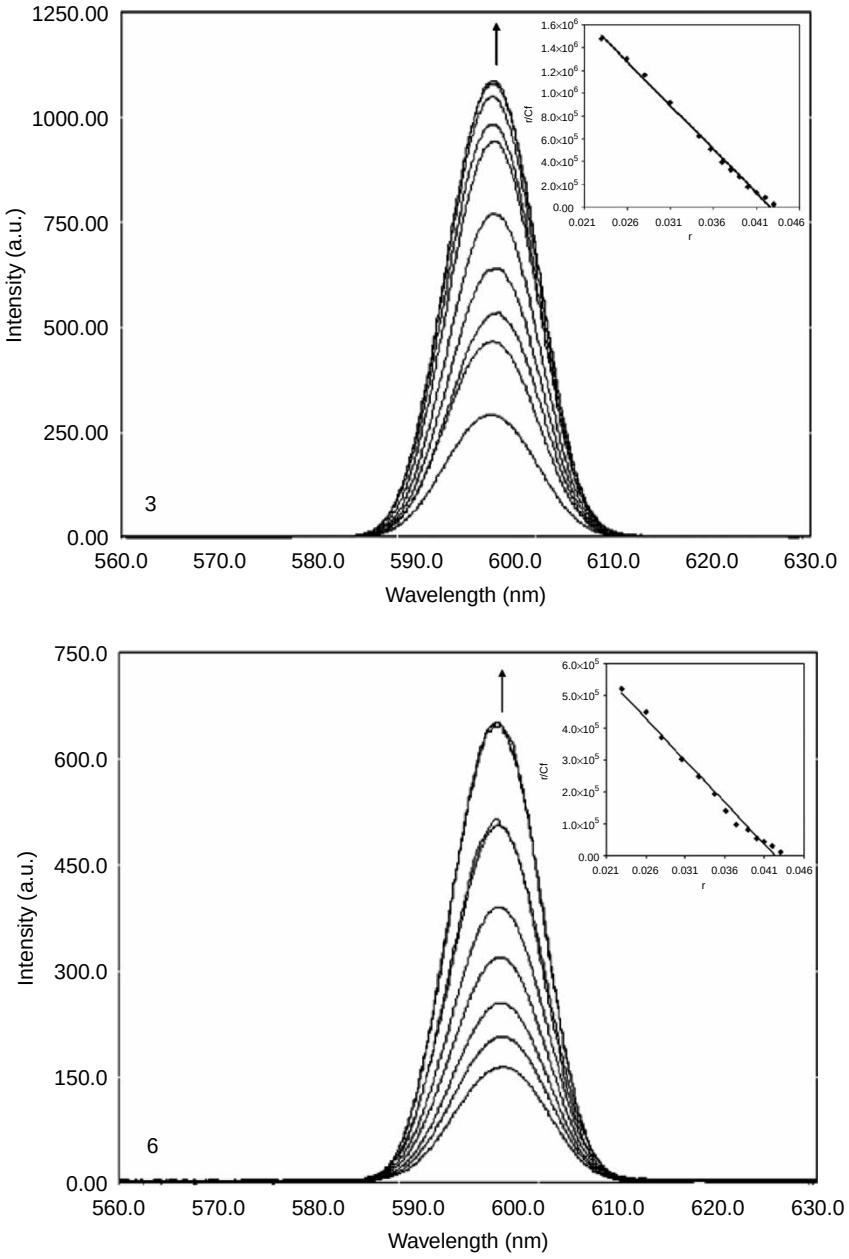

Figure 4. Emission spectra of complexes of $[Ru(phen)_2FIPC]^{2+}$(3) and $[Ru(phen)_2ClIPC]^{2+}$(6) in Tris–HCl buffer at 25°C upon addition of CT-DNA, [Ru] = 20 μM, [DNA] = 0–200 μM. The arrow shows the increase in intensity upon increasing CT-DNA concentrations.

DNA are shown in Figure 6. The viscosity measurement is based on the flow rate of a DNA solution through a capillary viscometer. The specific viscosity contribution (η) due to the DNA in the presence of a complex was obtained. As can be seen, there is a positive change in viscosity with increasing addition of the concentration of the complexes to DNA. These results suggested that all the complexes intercalated between two adjacent base pairs of DNA through a classical intercalation mode. The results indicate that the absence and presence of metal complexes have a marked effect on the viscosity of the DNA. The effects of complexes 1–6 and EtBr on the viscosity of rod-like DNA. EtBr is a known DNA intercalator and increases the relative specific viscosity by lengthening of the DNA double helix through the intercalation mode. Upon increasing the amounts of complexes 1–6, the relative viscosity of DNA increases steadily, similar to the behaviour of EtBr. Though the intercalating ligand is the same in all complexes, there is a small difference in the viscosity, this is due to the

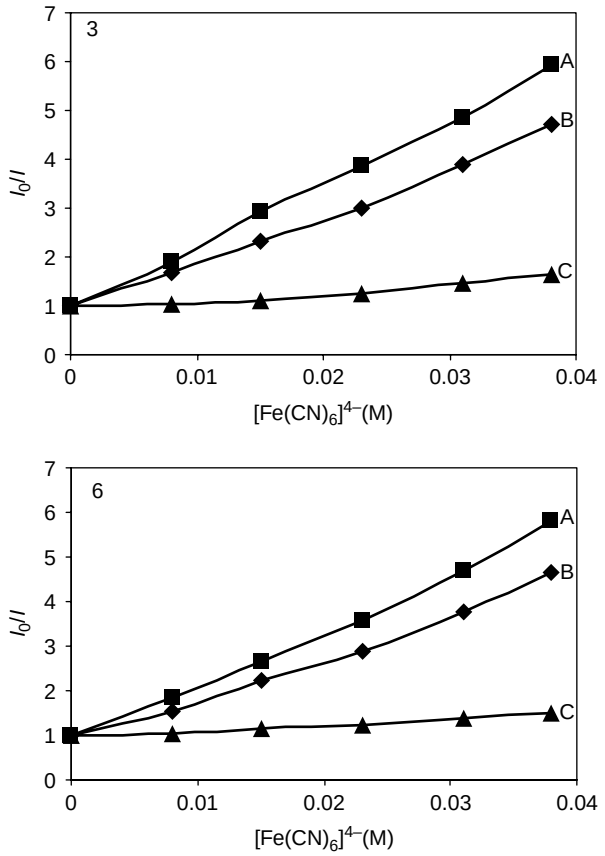

Figure 5. Emission quenching of complexes of $[Ru(phen)_2FIPC]^{2+}$(3), $[Ru(phen)_2ClIPC]^{2+}$(6) in the absence (A), presence (B) [DNA] = 0–200 μM, [Ru] = 20 μM and excess of DNA (C) [DNA] = 400 μM.

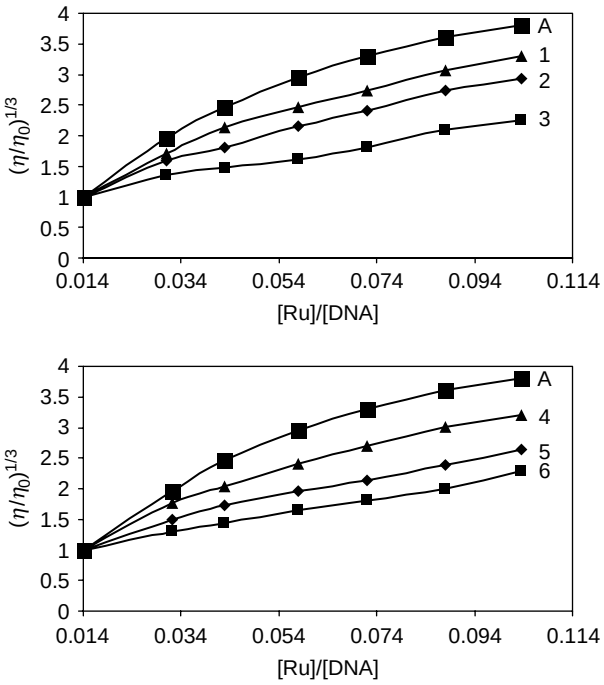

Figure 6. Effect of increasing amount of EtBr (A) $[Ru(bipy)_2FIPC]^{2+}$(1), $[Ru(dmb)_2FIPC]^{2+}$(2), $[Ru(phen)_2FIPC]^{2+}$(3), $[Ru(bipy)_2ClIPC]^{2+}$(4), $[Ru(dmb)_2ClIPC]^{2+}$(5) and $[Ru(phen)_2ClIPC]^{2+}$(6) on relative viscosity of CT-DNA at 30 ± 0.1°C. The total concentration of DNA is 0–200 μM, [Ru] = 20 μM.

difference in the ancillary ligands. These further suggest that six Ru(II) complexes show an intercalative binding mode to CT-DNA, which parallel the absorption titration results. The increased degree of viscosity, which may depend on the affinity for DNA, follows the order EB $>3>6>1>4>2>5$.

Effect of NaCl salt

The effect of salt cation on the complex-DNA adduct is shown in Figure 7. With increasing concentration of NaCl, the fluorescence intensity of the complex-DNA system decreases. With increasing concentration of NaCl, the fluorescence intensity decreased, consistent with the results obtained from EtBr and other DNA fluorescence probes. The decrease in fluorescence intensity with increasing salt concentration clearly tells the dependence of binding constant upon Na^+ concentration. This is a consequence of the linkage of ligand and Na^+ binding to DNA and may be analysed by polyelectrolyte theory. At higher Na^+ concentrations, the difference in the relative binding affinities of these four complexes and proven intercalators is more pronounced. These complexes would bind to DNA with an affinity of the order of $10^4\,M^{-1}$, whereas EtBr and daunomycin bind with an affinity of 10^5–$10^6\,M^{-1}$. Compared to proven intercalators these complexes form weak complexes with DNA. These complexes appear to be

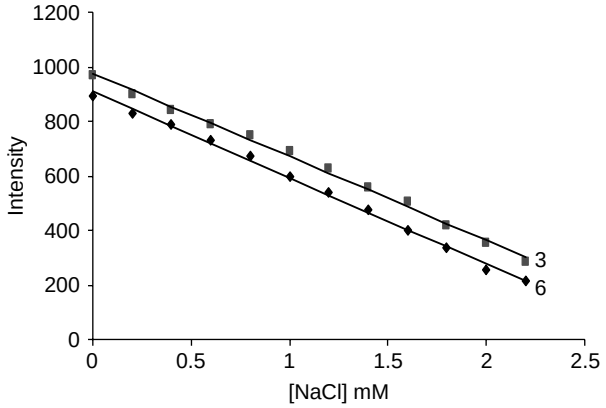

Figure 7. Curve representing the effect of NaCl on the fluorescence intensity of complexes $[Ru(phen)_2FIPC]^{2+}$(3), $[Ru(phen)_2ClIPC]^{2+}$(6) in Tris buffer solution (pH 7.1). The concentration of complexes was 1×10^{-4} mol/l, and that of DNA is 20 μl.

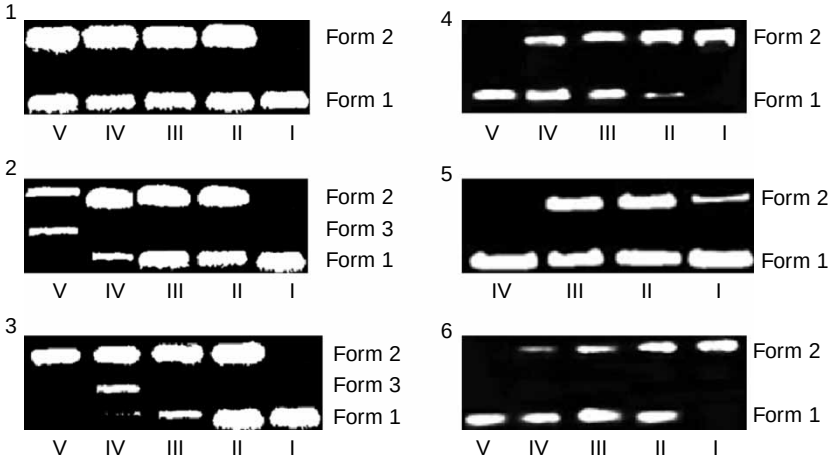

Figure 8. Photo-activated cleavage of pBR-322 DNA in the presence of $[Ru(bipy)_2FIPC]^{2+}$(1), $[Ru(dmb)_2FIPC]^{2+}$(2), $[Ru(phen)_2FIPC]^{2+}$(3), $[Ru(bipy)_2ClIPC]^{2+}$(4), $[Ru(dmb)_2ClIPC]^{2+}$(5) and $[Ru(phen)_2ClIPC]^{2+}$(6) and after 120 min irradiation at 365 nm. DNA alone (lane I), the concentrations of each complex was 20, 40, 60, 80 μM (lanes II–V).

intercalators based on viscosity studies but are not as good as proven intercalators.

Photo-activated cleavage of pBR-322 DNA by Ru(II) complexes

The cleavage of plasmid DNA can be monitored by agarose gel electrophoresis. In the dark, the complexes do not promote DNA strand breaks. Figure 8 shows gel electrophoretic separation of pBR-322 DNA after incubation with the complexes and irradiation at 365 nm. When the plasmid was irradiated in the presence of complexes, an efficient photo-induced DNA-strand cleavage occurs. When circular plasmid DNA is subjected to electrophoresis, relatively fast migration will be observed for the intact super coil form (Form 1). If scission occurs on one strand (nicking), the super coil will relax to generate a slower-moving open circular form (Form 2), if both strands are cleaved, a linear form (Form 3) that migrates between Form 1 and Form 2 will be generated (*48*). No DNA cleavage was observed for controls in which complexes were absent (lane I). At low concentrations of the complexes, no significant cleavage of the plasmid DNA was observed. With increasing concentration of the complexes (1–3; lanes II–V), (4–6; lanes II–V), a significant nicking of the super coiled plasmid form took place. The amount of the super coiled form of pBR-322 DNA diminishes gradually, whereas the movement of the nicked, slower moving open circular form increases (*48*). Under comparable experimental conditions, complexes 3 and 6 exhibit more effective DNA cleavage activity than other four complexes, as these two complexes bind strongly and intercalates more than other complexes. To identify the nature of the reactive species responsible for photo-activated cleavage of plasmid DNA, we have further investigated with the potentially $^1O_2$ inhibiting agent, histidine. Figure 9 shows the photoactivated cleavage of pBR-322 DNA in the presence of complex alone and complex with histidine. Indeed, plasmid DNA cleavage by complexes 1–6 was inhibited in the presence of histidine, which indicated that $^1O_2$ acts as a competing cleavage agent. In presence of histidine, Form 2 is not observed.

DNA melting studies

As intercalation of the complexes into DNA base pairs causes stabilisation of base stacking and hence raises the melting temperature of the double stranded DNA, the DNA

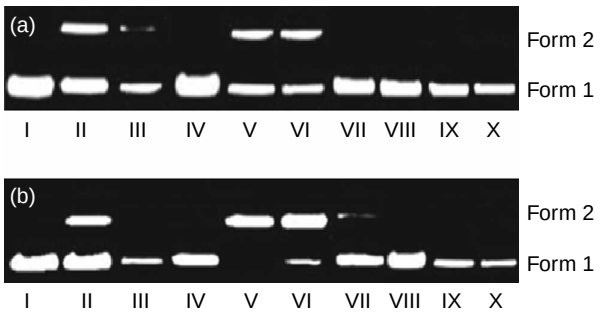

Figure 9. Photo-activated cleavage of pBR-322 DNA in the presence of $[Ru(bipy)_2FIPC]^{2+}$(1), $[Ru(dmb)_2FIPC]^{2+}$(2), $[Ru(phen)_2FIPC]^{2+}$(3), $[Ru(bipy)_2ClIPC]^{2+}$(4), $[Ru(dmb)_2ClIPC]^{2+}$(5) and $[Ru(phen)_2ClIPC]^{2+}$(6) and after 120 min irradiation at 365 nm. DNA alone (lane I), the concentrations of each complex was 20, 40, 60 μM (lanes II–IV $[Ru(bipy)_2FIPC]^{2+}$, $[Ru(bipy)_2ClIPC]^{2+}$; lanes V–VII $[Ru(dmb)_2FIPC]^{2+}$, $[Ru(dmb)_2ClIPC]^{2+}$ and lanes VIII–X $[Ru(phen)_2FIPC]^{2+}$, $[Ru(phen)_2ClIPC]^{2+}$), the concentration of the histidine inhibitor was 1.0, 2.0 mM. (Lanes III, IV, VI, VII, IX, X are in presence of histidine.)

Table 5. Results of absorption titration, thermal melting and fluorescence experiment.

Complexes	T_M (°C)	Hypochromicity (%)	Absorption λ_{max} (nm) Free	Bound	$\Delta\lambda$ (nm)	Absorption K_b (M^{-1})	F_{max}/F_0	Emission K_b (M^{-1})
CT DNA alone	62	–	–	–	–	–	–	–
$[Ru(bipy)_2FIPC]^{2+}$	68	12.5	446.0	454.0	8.0	$7.5 \pm 0.1 \times 10^4$	3.80	$8.5 \pm 0.1 \times 10^4$
$[Ru(dmb)_2FIPC]^{2+}$	66	9.2	453.5	458.5	5.0	$5.9 \pm 0.1 \times 10^4$	3.40	$6.1 \pm 0.1 \times 10^4$
$[Ru(phen)_2FIPC]^{2+}$	70	14.6	438.5	451.0	12.5	$9.0 \pm 0.1 \times 10^4$	4.20	$9.2 \pm 0.1 \times 10^4$
$[Ru(bipy)_2ClIPC]^{2+}$	66	10.6	446.0	453.5	7.5	$6.8 \pm 0.1 \times 10^4$	3.50	$7.2 \pm 0.1 \times 10^4$
$[Ru(dmb)_2ClIPC]^{2+}$	65	9.0	446.0	451.0	5.0	$5.5 \pm 0.1 \times 10^4$	3.20	$5.8 \pm 0.1 \times 10^4$
$[Ru(phen)_2ClIPC]^{2+}$	69	12.8	438.5	448.5	10.0	$8.6 \pm 0.1 \times 10^4$	4.00	$8.8 \pm 0.1 \times 10^4$

melting experiments are useful in establishing the extent of intercalation. All the three complexes were incubated with CT-DNA, heated to 85°C from ambient temperature, and the OD at 260 nm was monitored. Binding of complexes does lead to an increase in ΔT_m of DNA, in the order $3 > 6 > 1 > 4 > 2 > 5$ (Table 5).

Antimicrobial activity

The antifungal activity data (Table 6) indicate that the complexes show an appreciable activity against *A. niger* at 1.5 mg/ml concentration. DMSO control has shown a negligible activity as compared to the metal complexes. The experimental results of the compounds were compared against DMSO as the control and are expressed as inhibition zone diameter (in mm) vs. control. The complexes are more effective against *A. niger*. $[Ru(phen)_2FIPC]^{2+}$ and $[Ru(phen)_2ClIPC]^{2+}$ complexes show the highest activity (17 and 20 mm) against *A. niger* at the concentration of 1.5 mg/ml among all the metal complexes. The same metal complex exhibited greater antifungal activity against *A. niger* as compared to the standard drug flucanazole (15–18 mm). The complexes $[Ru(bipy)_2FIPC]^{2+}$(1), $[Ru(dmb)_2FIPC]^{2+}$(2), $[Ru(bipy)_2ClIPC]^{2+}$(4) and $[Ru(dmb)_2ClIPC]^{2+}$(5) show less activity against these fungi than the standard drug, flucanazole (15–18 mm).

The antibacterial activity data (Table 6) indicate that the complexes show a high activity against *B. subtilis* (G^+), *S. aureus* (G^+), *E. coli* (G^-) and *K. pneumoniae* (G^-) at 1 mg/ml concentration. DMSO control has shown a negligible activity as compared to the metal complexes. The experimental results of the compounds were compared against DMSO as the control and are expressed as inhibition zone diameter (in mm) vs. control. The complexes are more effective against *S. aureus, B. subtilis* than *E. coli* and *K. pneumoniae*. $[Ru(phen)_2FIPC]^{2+}$ and $[Ru(phen)_2ClIPC]^{2+}$ complexes show the highest activity of inhibition 21 and 20 mm against *S. aureus,* 21 mm inhibition against *B. subtilis* at the concentration of 1 mg/ml among all the metal complexes. The same complexes also show an activity of 18 mm inhibition against *E. coli*, and 18 and 17 mm inhibition against *K. pneumoniae*. The same metal complex exhibited greater antibacterial activity against *S. aureus* as compared to the standard drug streptomycin (13–17 mm). The complexes 1–5 show less activity against these bacteria than the standard drug, streptomycin. It is clearly evident from our results that all the metal complexes possess antifungal and antibacterial activity. It is also notable that compounds

Table 6. Antimicrobial activity of the Ru(II) complexes.

Complex	Bacterial species: Gram '+'ve *S. aureus*	*Bacillus*	Gram '−'ve *E. coli*	*K. pneumoniae*	Fungal species *A. niger*
Inhibition zone diameter(in mm)					
$[Ru(bipy)_2FIPC]^{2+}$	13	12	11		13
$[Ru(dmb)_2FIPC]^{2+}$	12	12	10	10	11
$[Ru(phen)_2FIPC]^{2+}$	21	21	18	18	19
$[Ru(bipy)_2ClIPC]^{2+}$	12	10	10	12	13
$[Ru(dmb)_2ClIPC]^{2+}$	10	11	12	12	10
$[Ru(phen)_2ClIPC]^{2+}$	20	21	18	17	20
Flucanazole	–		–		15–18
Streptomycin	13–17		13–17		–

1–6 can be potent antibacterial for the Gram + ve as well as Gram – ve organism. The enhancement of activity can be on the basis of chelation or may be due to overtone's concept (*49*, *50*). Chelation can considerably reduce the polarity of the metal ion, which in turn increases the lipophilic character of the chelate. Thus, the interaction between metal ion and lipid is favoured. This may lead to the breakdown of the permeability barrier of the cell, resulting in interference with the normal cell process. Some important factors that contribute to the activity are the nature of the metal ion, the nature of the ligand, coordinating sites and geometry of the complex, concentration, hydrophilicity, lipophilicity and the presence of co-ligands. Heterocyclic ligands with multifunctionality have a greater chance of interaction either with nucleoside bases and can be promising candidates as bactericides. Thus, the antibacterial property of metal complexes cannot be ascribed to chelation alone but it is an intricate blend of all the above contributions.

Conclusion

In summary, Ru(II) complexes $[Ru(bipy)_2FIPC]^{2+}$(1), $[Ru(dmb)_2FIPC]^{2+}$(2), $[Ru(phen)_2FIPC]^{2+}$(3), $[Ru(bipy)_2ClIPC]^{2+}$(4), $[Ru(dmb)_2ClIPC]^{2+}$(5) and $[Ru(phen)_2ClIPC]^{2+}$(6) have been synthesised and characterised. Their DNA-binding and photocleavage properties were also investigated. Interaction of pBR-322 DNA to the complexes is a typical example of intercalative mode. The electrophoresis experiment showed that the interaction of the complexes with DNA induces strand breakages. Spectroscopic studies and viscosity experiments supported that the complexes can intercalate into DNA base pairs via FIPC, ClIPC ligands. When irradiated at 365 nm, three Ru(II) complexes are efficient photocleavers of the plasmid pBR-322 DNA. Complexes 3 and 6 are found to show activity slightly more than the standard drugs against bacterial species.

References

(1) Nordén, B.; Lincoln, P.; Kerman, B.A.; Tuite, E. In *Metal Ions in Biological System*; Sigel, A., Sigel, H., Eds.; Marcel Dekker: New York, 1996; pp 177–252.
(2) Ramakrishnan, S.; Palaniandavar, M. *J. Chem. Sci* **2005**, *117*, 179–186.
(3) Lu, P.; Zhu, M.L.; Yang, P. *J. Inorg. Biochem*. **2003**, *95*, 31–36.
(4) Hemmert, C.; Pitie, M.; Renz, M.; Gornitzka, H.; Meunier, S.B. *J. Biol. Inorg. Chem.* **2001**, *6*, 14–22.
(5) Navarro, M.; Cisneros-Fajardo, E.J.; Sierralta, A.; Fernadez-Mastre, M.; Silva, P.; Arrieche, D.; Marchan, E. *J. Biol. Inorg. Chem.* **2003**, *8*, 401–408.
(6) Zhang, Q.-L.; Liu, J.-G.; Chao, H.; Xue, G.-Q.; Ji, L.-N. *J. Inorg. Biochem.* **2001**, *83*, 49–55.
(7) Liu, J.-G.; Zhang, Q.-L.; Ji, L.-N. *Transition Met. Chem*. **2001**, *26*, 733–738.
(8) Jiang, C.-W.; Chao, H.; Li, H.; Ji, L.-N. *J. Inorg. Biochem* **2003**, *93*, 247–255.
(9) Vaidyanathan, V.G.; Nair, B.U. *J. Chem. Soc. Dalton Trans.* **2005**, *17*, 2842–2848.
(10) Chao, H.; Mei, W.-J.; Huang, Q.-W.; Ji, L.-N. *J. Inorg. Biochem.* **2002**, *92*, 165–170.
(11) Jiao, K.; Wang, Q.-X.; Sun, W.; Jian, F.F. *J. Inorg. Biochem.* **2005**, *99*, 1369–1375.
(12) Satyanarayana, S.; Dabrowiak, J.C.; Chaires, J.B. *Biochemistry* **1993**, *32*, 2573–2584.
(13) Coury, J.E.; Anderson, J.R.; McFail-Isom, L.; Williams, L.D.; Battenly, L.A. *J. Am. Chem. Soc.* **1997**, *119*, 3792–3796.
(14) Liu, X.W.; Li, J.; Li, H.; Zheng, K.C.; Chao, H.; Ji, L.N. *J. Inorg. Biochem.* **2005**, *99*, 2372–2380.
(15) Liu, Y.J.; Wei, X.Y.; Mei, W.J.; He, L.X. *Transition Met. Chem.* **2007**, *32*, 762–768.
(16) Tan, L.F.; Chao, H. *Inorg. Chim. Acta* **2007**, *360*, 2016–2022.
(17) Liu, J.G.; Ye, B.H.; Li, H.; Zhen, Q.X.; Ji, L.N. *J. Inorg. Biochem.* **1999**, *76*, 265–271.
(18) Terbrueggen, R.H.; Johann, T.W.; Barton, J.K. *Inorg. Chem.* **1998**, *37*, 6874–6883.
(19) Franklin, S.J.; Barton, J.K. *Biochemistry* **1998**, *37*, 16093–16105.
(20) Liu, J.G.; Zhang, Q.L.; Shi, X.F.; Ji, L.N. *Inorg. Chem.* **2001**, *40*, 5045–5050.
(21) Maheswari, P.U.; Rajendiran, V.; Palaniandavar, M.; Parthasarathi, R.; Subramanian, V. *J. Inorg. Biochem.* **2006**, *100*, 3–17.
(22) Biver, T.; Cavazza, C.; Secco, F.; Venturini, M. *J. Inorg. Biochem.* **2007**, *101*, 461–469.
(23) Ashwini Kumar, K.; Laxma Reddy, K.; Vidhisha, S.; Satyanarayana, S. *Appl. Organometal. Chem.* **2009**, *23*, 409–420.
(24) Laxma Reddy, K.; Harish Kumar Reddy, Y.; Ashwini Kumar, K.; Vidhisha, S.; Satyanarayana, S. *Nucleosides Nucleotides Nucleic Acids* **2009**, *28*, 204–219.
(25) Nagababu, P.; Satyanarayana, S. *Polyhedron* **2007**, *26*, 1686–1692.
(26) Nagababu, P.; Aravind Kumar, D.; Reddy, K.L.; Ashwini Kumar, K.; Mustafa, Md.B.; Shilpa, M.; Satyanarayana, S. *Metal-Based Drugs* **2008**, Article ID 275084, 8 pages.
(27) Pallavi, P.; Nagababu, P.; Satyanarayana, S. *Helvetica Chem. Acta* **2007**, *90*, 627–639.
(28) Perrin, D.; Annarego, W.L.F.; Perrin, D.R. *Purification of Laboratory Chemicals*;, 2nd ed. Pergamon Press: New York, 1980.
(29) Marmur, J. *Mol. J. Biol.* **1961**, *3*, 208–218.
(30) Rreichmann, M.F.; Rice, S.A.; Thomas, C.A.; Doty, P. *J. Am. Chem. Soc.* **1954**, *76*, 3047–3053.
(31) Yamada, M.; Tanaka, Y.; Yoshimoto, Y.; Kuroda, S.; Shimo, I. *Bull. Chem. Soc. Jpn* **1992**, *65*, 1006–1011.
(32) Sullivan, B.P.; Salmon, D.J.; Mayer, T.J. *Inorg. Chem.* **1978**, *17*, 3334–3341.
(33) Chaires, J.B.; Dattaguptha, N.; Crother, D.M. *Biochemistry* **1982**, *21*, 3933–3940.
(34) Drew, W.L.; Barry, A.L.; O'Toole, R.; Sherris, J.C. *Appl. Environ. Microbiol.* **1972**, *24*, 240–247.
(35) Moucheron, C.; Mesmaeker, A.K.D.; Choua, C. *Inorg. Chem.* **1997**, *36*, 584–592.
(36) Pyle, A.M., Barton, J.K., Lippard, S.J., Eds.; *Progress in Inorganic Chemistry: Bioinorganic Chemistry*; Wiley: New York, 1990; Vol. 38, pp 413–475.
(37) Chen, H.-L.; Yang, P. *Chin. J. Chem.* **2002**, *20*, 1529.

(38) Wolfe, A.; Shimer, G.H., Jr. Meehan, T. *Biochemistry* **1987**, *26*, 6392–6396.
(39) Gao, F.; Chao, H.; Zhou, F.; Yuan, Y.X.; Peng, B.; Ji, L.N. *J. Inorg. Biochem.* **2006**, *100*, 1487–1494.
(40) Liu, Y.J.; Chao, H.; Yuan, Y.X.; Yu, H.J.; Ji, L.N. *Inorg. Chim. Acta* **2006**, *359*, 3807–3814.
(41) Liu, Y.-J.; He, J.-F.; Yao, J.-H.; Mei, W.-J.; Haiwu, F.; He, L.-X. *J. Coordinat. Chem.* **2009**, *62*, 665–675.
(42) McGhee, J.D.; Von Hippel, P.H. *J. Mol. Biol.* **1974**, *86*, 469.
(43) Wu, J.; Du, F.; Zhang, P.; Khan, I.A.; Chen, J.; Liang, Y. *J. Inorg. Biochem.* **2005**, *99*, 1145.
(44) Zhen, Q.-X.; Ye, B.-H.; Zang, Q.-L.; Liu, J.-G.; Li, H.; Ji, L.-N.; Wang, L. *J. Inorg. Biochem.* **2000**, *78*, 293–298.
(45) Lakowicz, J.R.; Webber, G. *Biochemistry* **1973**, *12*, 4161–4170.
(46) Satyanarayana, S.; Dabrowiak, J.C.; Chaires, J.B. *Biochemistry* **1992**, *31*, 9319–9324.
(47) Sigman, D.S.; Mazumder, A.; Perrin, D.M. *Chem. Rev.* **1993**, *93*, 2295–2316.
(48) Barton, J.K.; Raphael, A.L. *J. Am. Chem. Soc.* **1984**, *106*, 2466–2468.
(49) Kumar, R.S.; Arunachalam, S.; Periasamy, V.S.; Preethy, C.P.; Riyasdeen, A.; Akbarsha, M.A. *Aust. J. Chem.* **2009**, *62*, 165–175.
(50) Abu-Melha, K.S.; EI-Metwally, N.M. *Transition. Met. Chem.* **2007**, *32*, 828–834.